

Influence of Environmental Temperature on the Electrochemical Performance of a Tin-Based Nano-Electrode in Lithium Ion Cells

G. Kilibarda^{1,2,*}, S. Schlabach¹, T. Hanemann^{1,2}, D.V. Szabó¹

¹Karlsruhe Institute of Technology, Institute for Applied Materials, Germany

²University of Freiburg, Department of Microsystems Engineering, Germany

*E-mail: goran.kilibarda@kit.edu

Received: 21 February 2013 / Accepted: 29 March 2013 / Published: 1 May 2013

Tin-carbon-composite-nanoparticle layer electrodes were synthesized by the KMPP consisting of spherical Sn-nanoparticles and carbonaceous material with a particle size below 10 nm. Electrochemical measurements were performed in environmental temperatures of 0 °C, RT, 40 °C, 60 °C. It was shown that with elevating temperature the capacities and the degradation increase while the columbic efficiency decrease. The reasons for this temperature behavior can be explained by the Arrhenius equation, electrical and ionic conductivity of the electrolyte, the ohmic and the diffusion overpotentials.

Keywords: Li-ion battery, Sn nanocomposite electrode, temperature, electric and ionic electrolyte conductivity, ohmic and diffusion overpotential

1. INTRODUCTION

Lithium-ion batteries have been commercially used for a number of years in small portable devices. Nowadays, for example the automotive industry is looking for new systems combining electro motors with lithium ion batteries as a storage medium. Because the vehicles are exposed to several external conditions, batteries must withstand temperatures between minus and plus degrees. It is known that the performance of lithium-ion cells is strongly dependent on the environmental temperature. Some studies have been conducted which indicate that the temperature has a severe influence on the specific capacity and that elevated temperature causes an increases in degradation of these capacities. Studies on cathode materials LiFePO₄ [1], Li[Li_{0.2}Co_{0.4}Mn_{0.4}]O₂ [2] or batteries using anodes, as LMAOF/carbon [3], graphite in combination with LiPF₆ [4], Li-Ni_{0.8}Co_{0.15}Al_{0.05}/graphite

[5] and Sony 18650 cells [6], have been done. Temperature-cyclic-investigations on tin-based electrodes in combination with LiPF_6 in 50:50 EC/DMC, to our best knowledge, were not proposed in literature, yet. As Sn-based materials are promising for anodes [7, 8], this work investigates the temperature influence on specific capacity of a tin-based nano-electrode in a lithium half-cells.

2. EXPERIMENTAL PART

Tin-carbon-composite-nanoparticle layer based electrodes without conventional slurry processing were made *in-situ* by Karlsruhe Microwave Plasma Process (KMPP). Details of the process are described elsewhere [9]. Water-free tetra-n-butyltin, $\text{Sn}(\text{C}_4\text{H}_9)_4$ (94%, ABCR, Karlsruhe, Germany), was used as precursor for the synthesis of Sn (feeding rate of 5 ml h^{-1}). Pure Ar was used as reaction gas (gas flow 5 l min^{-1}). The microwave power was set to 700 W, and the system pressure to 13 mbar. Under the selected experimental conditions, the precursor was expected yielding metallic Sn nanoparticles and a carbonaceous residual. For the utilization as negative electrode material, the reaction product has been deposited *in-situ* as a porous nanoparticle film on $300 \text{ }^\circ\text{C}$ preheated Ni-substrates, which act as the current collector. Swagelok-type half-cells were assembled in an argon-filled Unilab glove box (MBraun, Garching, Germany). The electrodes, consisting of the *in-situ* deposited tin-carbon-composite nanoparticle film, were used without any additional carbon-black or binder, and heated in the glove box for 2 h at $140 \text{ }^\circ\text{C}$ to get rid of moisture [9]. A glass fiber (Whatman, Maidstone, England) was used as separator. Lithium foil (99.9%, Alfa-Aesar, Ward-Hill, USA) was used as counter and reference electrode. The electrolyte consisting of a solution of 1 M LiPF_6 in ethylene-carbonate (EC) and dimethyl-carbonate (DMC) (50:50) was obtained from Merck (LP 30, Merck, Darmstadt, Germany). Altogether, three Swagelok-cells were treated electrochemically in the same way. As they show the same behavior, the results of one of these cells will be discussed in detail exemplary for all.

The anode material (nanoscaled composite powder) was characterized by X-ray diffraction (XRD, Philips-X'Pert, PANalytical, Almelo, The Netherlands) and by transmission electron microscopy (TEM, Tecnai F20ST, FEI, Eindhoven, The Netherlands).

Long term cycling measurements were done using a Lithium cell cycler (KIT, IPE, Germany) in the voltage range of 0.1 - 2.8 V (vs. Li^+/Li) at a constant current density of 49 mA g^{-1} . During the whole cycling the cells were placed either in a drying oven (Heraeus T6060, Thermo-Electron-LED, Langensfeld, Germany) at a given temperature or in a modified conventional refrigerator. The electrochemical measurement process was set up as follows:

- 14 cycles in the drying oven at $40 \text{ }^\circ\text{C}$
- unsupported cooling to room temperature (RT) and cycling for 4 cycles at RT
- raising of temperature to $40 \text{ }^\circ\text{C}$ with $4 \text{ }^\circ\text{C min}^{-1}$, cycling for 10 cycles. For closer examination, the changing point in the 19th cycle was performed exactly at a voltage of 0.13 V in the discharging process, so that with ongoing discharging the change in specific capacity with potential is directly observable.

- 4 cycles in a modified conventional refrigerator with an environmental temperature of 0 °C.
- 14 cycles in the drying oven with a temperature already set to 60 °C.
- finally, unsupported reduction of the environmental temperature to RT and cycling for 13 cycles. The changing point in the 47th cycle was performed exactly at 1.1 V during the discharging process, again, to allow closer examination of the ongoing discharging cycle.

3. RESULTS AND DISCUSSION

Microstructural and microanalytical investigation show that the material consists of spherical Sn-nanoparticles and carbonaceous material. Figure 1a shows a XRD image of the tetragonal tin-nanoparticles with the corresponding Miller indices [10] superimposed on a more amorphous-like phase.

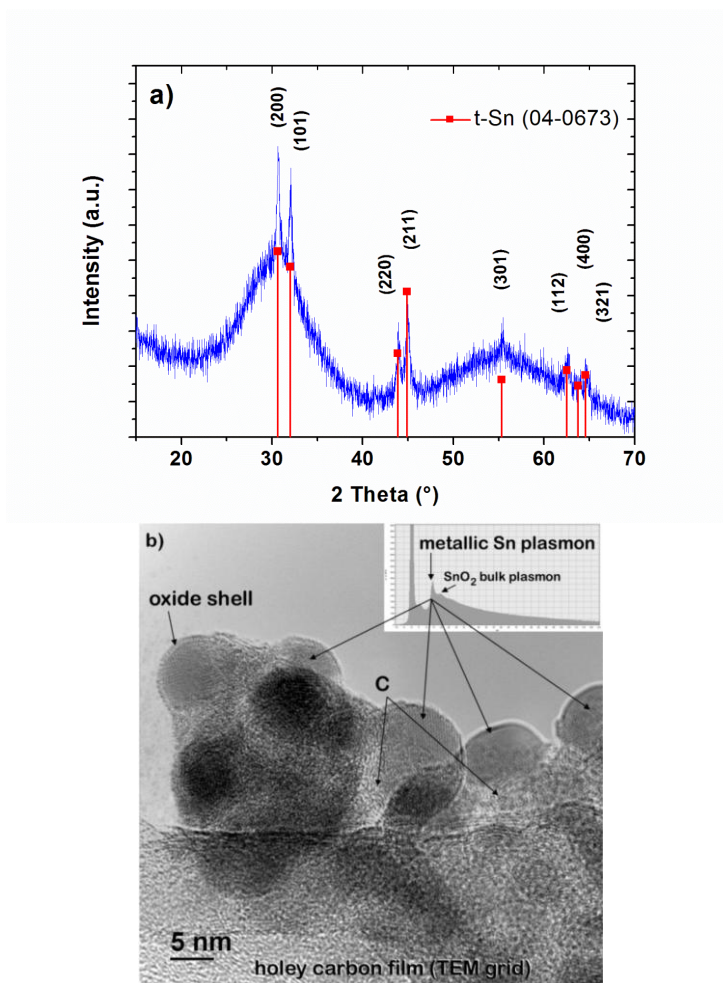


Figure 1 (a) XRD image showing tetragonal Sn nanoparticles with the corresponding Miller indices [10] superimposed on an amorphous-like phase (b) TEM image of the tetragonal Sn nanoparticles, the carbonaceous residual of the precursor and the EELS low loss spectrum

From the TEM image (Fig.1 b), a particle size below 10 nm can be estimated. Lattice fringes clearly show crystallinity of the Sn particles. The EELS low loss spectrum shows metallic tin bulk plasmon loss at ca. 14 eV, which is in good agreement to literature [11] and a small plasmon peak around 20 eV, indicating SnO₂ [12]. This plasmon loss may be due to atmospheric contamination of the sample. The carbonaceous residual of the precursor seems to be like a skinny amorphous layer.

The long term cycling measurements (Fig. 2) show, the specific capacity is strongly influenced by the environmental temperature. During the first change of temperature (decrease from 40 °C to RT) the specific capacity in the cell decreases from 1143 to 613 mAh g⁻¹. By increasing the temperature again to 40 °C the capacity rises from 619 to 1275 mAh g⁻¹. The subsequent reduction of temperature till 0 °C shows drastic capacity losses (from 874 to 173 mAh g⁻¹). A huge increase in capacity could be noted after raising the temperature to 60 °C (from 162 to 2620 mAh g⁻¹). The extremely huge capacities during 60 °C degraded much faster and after few cycles these capacities could be extrapolated to capacity values of 40 °C. Finally, after switching back to RT the capacity decreased again (from 744 to 283 mAh g⁻¹).

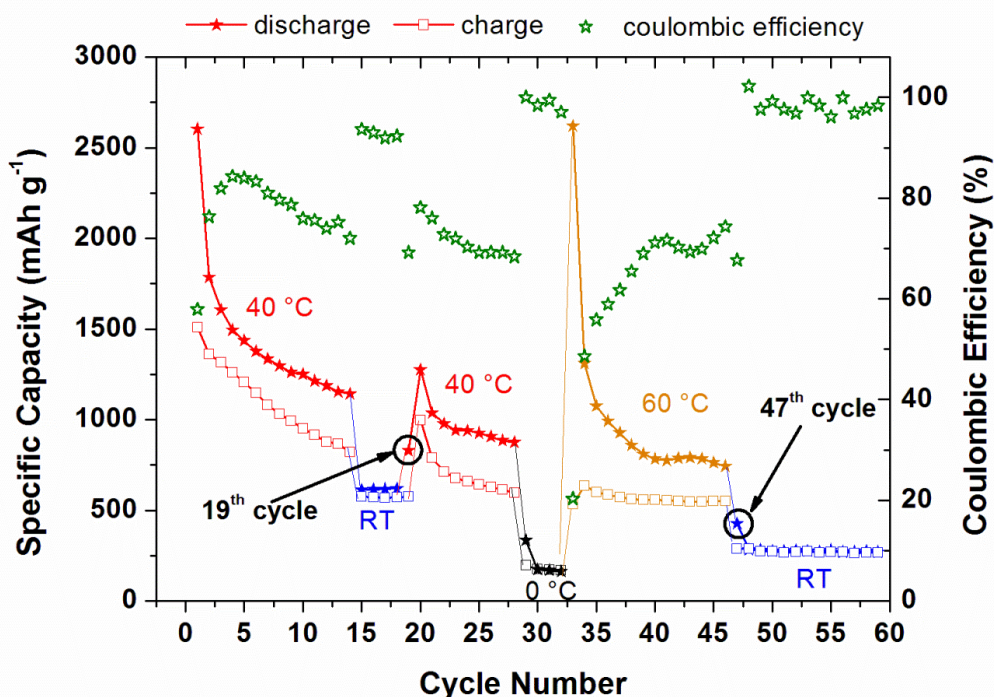


Figure 2. Long term cycling measurement of a Swagelok-cell under different thermal conditions

The degradation of specific capacity at 40 and 60 °C is much higher than that observed at RT and 0 °C. With higher capacities at elevated temperatures it can be assumed, that more Li⁺-ions are introduced in the electrode. Consequently, the mechanical stresses (volume changes) increase resulting in huger loss of active material and hence decreased capacity for the following cycles. Additionally, at elevated temperatures enhanced electrolyte decomposition (SEI formation) takes place [13]. In our previous work [14], XPS-measurements showed that even the SEI is increasing with cycling, so, on a long time scale, SEI penetrates into pores of the electrode and in addition may also penetrate into pores of the separator. This may result in a decreases of accessible surface areas due to this continuous SEI

growing [13]. Additionally, the SEI growth leads to an impedance rise [6, 13] and so all of this aspects increase the degradation of capacity for following cycles.

As can be seen, the irreversible capacity loss between the discharging and the charging process is higher at elevated temperatures (Fig. 2). That means the columbic efficiency at elevated temperature is much lower compared to RT and 0°C. This must be a result of an irreversible reaction in the reduction process of the high temperature stages (40 and 60°C). Therefore, however, the reaction in the discharging process consumes more Li⁺-ions than in the charging process. Probably the activation for side reactions on the process occurring in the solid phase, electrode-electrolyte interphase and in the electrolyte [6], which are irreversible formed only in the reduction process, increases with elevated temperature. One of these side reactions could be attributed to SEI formation.

Table 1. overview of reactions in the discharging and charging process, dependent on environmental temperature

	Discharging process (reduction)	Charging process (oxidation)
RT, 0°C	$\text{Sn} + x\text{Li}^+ + xe^- \rightarrow \text{Li}_x\text{Sn}$	$\text{Li}_x\text{Sn} \rightarrow \text{Sn} + x\text{Li}^+ + xe^-$
	$\text{Sn} + x\text{Li}^+ + xe^- \rightarrow \text{Li}_x\text{Sn}$	$\text{Li}_x\text{Sn} \rightarrow \text{Sn} + x\text{Li}^+ + xe^-$
40, 60 C	Numerous unknown side reactions occurring in the solid phase, electrode-electrolyte interphase and in the electrolyte due to elevated temperature [6] Exemplary one is solid electrolyte interface $\text{Electrolyte} + x\text{Li}^+ + xe^- \rightarrow \text{SEI}$	---

Generally, the discharging process starts at a potential of 2.8 V and at a potential of 0.1 V there is a dead center. The effects of temperature change are investigated closer starting at two specific points (highlighted marks in Fig. 2). The temperature change in the 19th cycle, preformed exactly at 0.13 V in the discharging process is characterized by an additional capacity increase of around 215 mAh g⁻¹ compared to the previous discharging (Fig 3a). The temperature change in the 47th discharge cycle, performed exactly at 1.1 V, exhibits a specific capacity loss of around 342 mAh g⁻¹ compared to the previous discharging cycles (Fig. 3b).

The observed increase of capacity with increasing temperature, and the decreasing capacity with decreasing temperature can be attributed to several reasons.

The first explanation is the temperature dependent rate of a reaction, described by Arrhenius equation.

$$k = A * \exp (-E_A / R * T) \tag{1}$$

Here k is the rate coefficient, A is a constant, E_A is the activation energy, R is the universal gas constant, and T is the temperature. This formula shows that the rate increases by increasing the temperature and so the chemical reactions may be faster. Hence, the specific capacity rises.

The second influencing factor is the electrical and ionic conductivity of the electrolyte, which is strongly influenced by the temperature. Namely, the electrical and ionic conductivity of this electrolyte increases with increasing temperature [4, 15] where viscosity of the solution is relatively low. Consequently, the specific capacity increases, too.

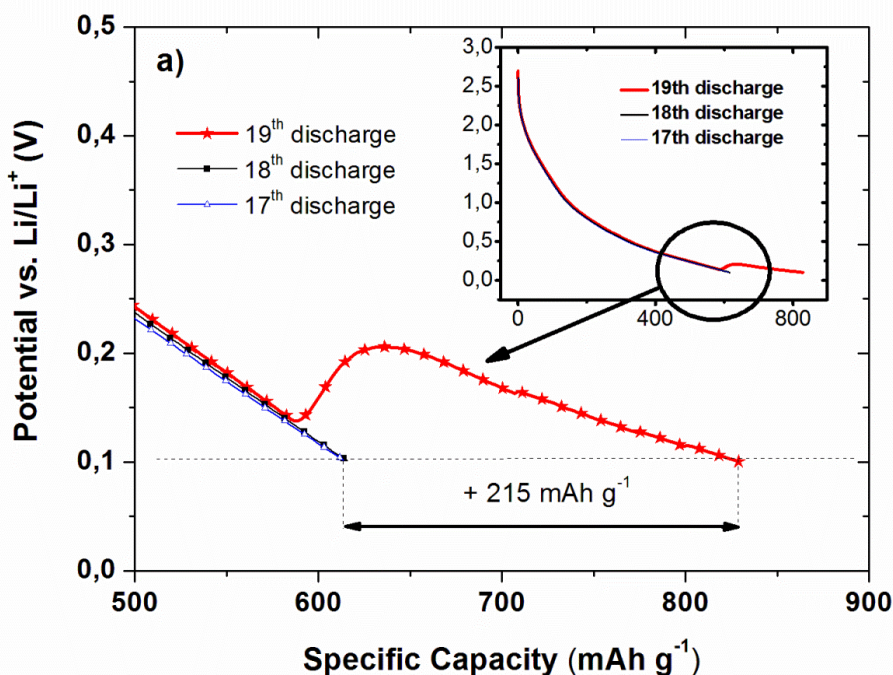
Finally, the electrochemical overpotential describes all potential drops taking place in a cell during cycling. The ohmic and the diffusion overpotentials are strongly influenced by the temperature.

- ohmic overpotential:

The electrical internal resistance R_i of a cell decreases with increasing temperature [6]. When lowering the internal resistance, according to Ohm's Law

$$E_{ohm} = R_i * I \tag{2}$$

the ohmic potential drop E_{ohm} decreases, too. The increase of temperature (Fig. 3a) causes a potential drop decrease, which actually means potential increase of the cell. In contrast, the decrease of temperature (Fig. 3b) results in electrical internal resistance increase, so that the potential drop increase leads to an additional capacity loss.



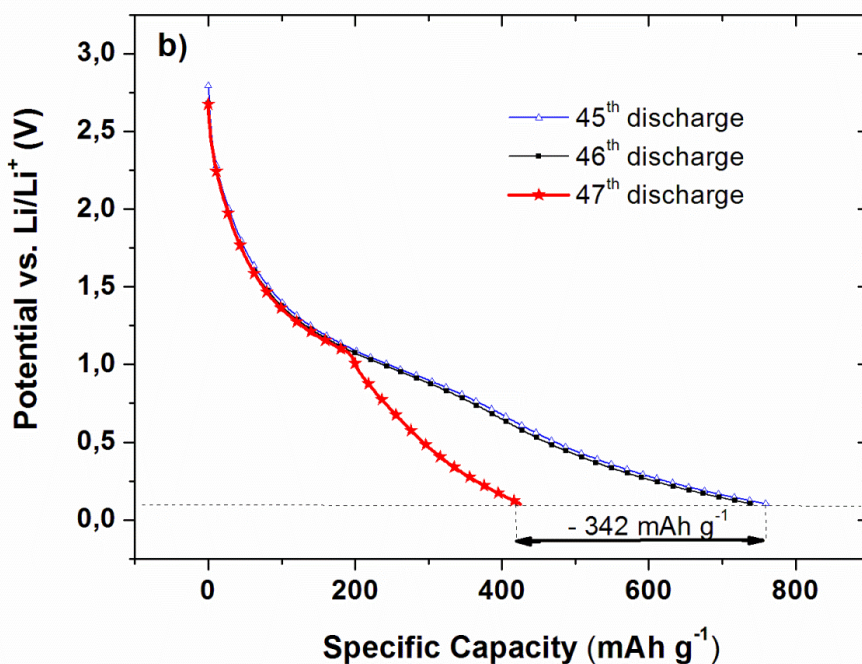


Figure 3. Detailed study of the specific capacity while temperature changes during a cycle. **a)** The temperature in the 19th discharging process was set exactly at a voltage of 0.13 V from RT to 40 °C. The capacity increases around 215 mAh g⁻¹. **b)** The temperature in the 47th discharging process was set exactly at a voltage of 1.1 V from 60 °C to RT. The capacity decreases about 342 mAh g⁻¹

- *diffusion overpotential:*

Between electrode and electrolyte, the Nernst diffusion layer acts as a diffusion barrier [16]. Here the kinetics of the electrochemical reaction is determined solely by diffusion. Due to this barrier, the concentration of the reacting product decreases. The smaller the concentration is, the smaller the amount of compounds that can react, therefore the potential drops (diffusion overpotential). With increasing temperature, the diffusion increases, too. Consequently, the concentration of the reacting product is less decreasing and the potential drop by diffusion (diffusion overpotential) decreases, too. As a result the potential of the cell increases (Fig. 3a) with increasing temperature and thus the specific capacity rises.

4. SUMMARY AND CONCLUSIONS

The Karlsruhe Microwave-Plasma-Process was used for the synthesis of tin-carbon-composite-nanoparticle layer based electrode without conventional slurry formation. Swagelok-type half-cells were assembled and long-term cycling measurements were performed at a constant current range of 49 mA g⁻¹. During these cycling measurements, the environmental temperature was changed between 0 and 60 °C. The specific capacity is found to be strongly dependent on the environmental temperature.

It was shown, that with increasing temperature, the specific capacity rises, too. In contrast, decreasing of environmental temperature causes capacity losses. The capacity change by temperature change can be explained by applying the Arrhenius equation, electrical and ionic conductivity of the electrolyte and changes of the ohmic and diffusion overpotentials. All of these points encourage the capacity-temperature behavior. The high temperature stages degrade faster, because the mechanical volume changes increases with elevated temperature, so the loss of active material, used for following cycles, increases. Additionally, the electrolyte decomposition (SEI formation) is reinforced by increasing temperature, so this may result in a decrease of accessible surface areas due to continuous SEI growing which reinforces the degradation. The difference of the coulombic efficiency between the high and the low temperature stages are attributed to irreversible reactions in the reduction process of the high temperature stage.

ACKNOWLEDGMENTS

We acknowledge support by Deutsche Forschungsgemeinschaft and Open Access Publishing Fund of Karlsruhe Institute of Technology.

References

1. A.S. Andersson, J.O. Thomas, B. Kalska, L. Häggström, *Electrochem. Solid State Lett.* 3 (2000) 66-68.
2. Z. Li, Y. Wang, X. Bie, K. Zhu, C. Wang, G. Chen, Y. Wei, *Electrochem. Commun.* 13 (2011) 1016-1019.
3. G. Amatucci, A. Du Pasquier, A. Blyr, T. Zheng, J.M. Tarascon, *Electrochim. Acta* 45 (1999) 255-271.
4. S.S. Zhang, K. Xu, T.R. Jow, *Electrochem. Commun.* 4 (2002) 928-932.
5. J. Shim, R. Kostecki, T. Richardson, X. Song, K.A. Striebel, *J. Power Sources* 112 (2002) 222-230.
6. P. Ramadass, B. Haran, R. White, B.N. Popov, *J. Power Sources* 112 (2002) 606-613.
7. Y. Idota, T. Kubota, A. Matsufuji, Y. Maekawa, T. Miyasaka, *Science* 276 (1997) 1395-1397.
8. A.R. Kamali, D.J. Fray, *Rev. Adv. Mater. Sci.* 27 (2011) 14-24.
9. D.V. Szabó, G. Kilibarda, S. Schlabach, V. Trouillet, M. Bruns, *Journal of Materials Science* 47 (2012) 4383-4391.
10. Joint Committee on Powder Diffraction Standards, Card N^o 4-0673 (tetragonal tin).
11. G.B. Hoflund, G.R. Corallo, *Phys. Rev. B* 46 (1992) 7110-7120.
12. R.A. Powell, *Appl. Surf. Sci.* 2 (1979) 397-415.
13. J. Vetter, P. Novák, M.R. Wagner, C. Veit, K.C. Möller, J.O. Besenhard, M. Winter, M. Wohlfahrt-Mehrens, C. Vogler, A. Hammouche, *J. Power Sources* 147 (2005) 269-281.
14. G. Kilibarda, D.V. Szabó, S. Schlabach, V. Winkler, M. Bruns, T. Hanemann, *J. Power Sources* 233 (2013) 139-147.
15. P.E. Stallworth, J.J. Fontanella, M.C. Wintersgill, C.D. Scheidler, J.J. Immel, S.G. Greenbaum, A.S. Gozdz, *J. Power Sources* 81-82 (1999) 739-747.
16. W.J. Moore, *Basic Physical Chemistry*, Prentice-Hall (1983).